Physica Scripta

PAPER

On the structure and icosahedral interconnectivity in Tantalum monatomic glass produced under pressure

RECEIVED
4 April 2024

REVISED
6 June 2024

ACCEPTED FOR PUBLICATION
3 July 2024

PUBLISHED
12 July 2024

Meryem Kbirou[1], **Achraf Atila**[2] **and Abdellatif Hasnaoui**[3]

[1] Laboratoire de Physique de la Matière Condensée, Faculté des Sciences Ben M'sik, University Hassan II of Casablanca, B.P 7955, Av Driss El Harti, Sidi Othmane, Casablanca, Morocco
[2] Department of Material Science and Engineering, Saarland University, Saarbrücken, 66123, Germany
[3] LS2ME, Faculté Polydisciplinaire Khouribga, Sultan Moulay Slimane University of Beni Mellal, B.P 145, 25000 Khouribga, Morocco

E-mail: kbiroumeryem@gmail.com

Keywords: medium range order, monatomic metallic glasses, icosahedral interconnectivity, high pressure, molecular dynamics simulations, short range order

Abstract

Proper processing of bulk metallic glasses (BMGs) under pressure is a promising approach to tailor their properties. However, to fully understand how pressure processing affect the final glass properties, a clearer understanding of how the pressure affects the structure of the glass at both short- and medium range levels is required. Accordingly, using molecular dynamics simulations, we study the effect of cooling under pressure on the local structure and the medium-range connectivity in a model Tantalum monatomic metallic glass. Crystalline grains form in the Ta sample with increasing the pressure under which the sample was cooled. These observations were confirmed by decreasing the fivefold symmetry with increasing pressure. The connectivity type between the perfect icosahedra was determined and showed that when cooled under pressure, intercross sharing is favored in the higher pressure. This work gives insights into understanding local structural changes induced by the pressure in metallic glasses.

Introduction

Metallic Glasses (MGs) are a new class of materials that have undergone a renaissance, with great potential in biomedical applications, as they are generally used for medical implants, surgical tools, and other bio-related devices[1–4]. Compared to their crystalline counterparts, they offer a great combination of properties, such as yield strength, ductility, toughness, ease of fabrication, and corrosion resistance [5]. These unique properties from mechanical to thermal and chemical properties of glasses, are evidenced from the unique characteristic of the glassy state, namely the absence of translational periodicity and compositional homogeneity, inducing the structure-properties relationship in MGs [6–12].

The response of glasses to increasing pressures is an area of research that interests many investigators in material science and condensed matter physics [13]. The structure and properties of glasses can be significantly influenced under high pressures, and studying glasses under higher pressures is important for the following reasons. First, the property of the higher chemical and mechanical durability of glasses manifested upon compression indicates that the formation of glasses under high pressure leads to potential technological applications [14]. Second, the application of high pressures in glasses such as oxide glasses have been proved to tune their physical properties reversibly or irreversibly, which improve the densification, including the elastic and plastic deformation of glasses [15–18]. Finally, high pressure can significantly enrich the glass formation by catalyzing the formation of many chemical species and promoting many new phenomena [13, 19–23].

In Bulk Metallic Glasses (BMGs), High Pressure (HP) is used to control the nucleation and growth, and thus, the BMG could be crystallized into very fine-grained nanostructural material under HP [24]. On the other hand, recent experiments from different groups have shown that applying external pressure to MGs results in significant glass rejuvenation, which is signaled by a substantial increase in the excess relaxation enthalpy and in

the decrease of the boson peak in the specific heat (where the boson peak represents an excess of low-energy vibrational states over the Debye law in the vibrational density of states) [19]. Structurally, substantial efforts have been devoted to understand the Short and Medium-Range Order (SRO) and (MRO) structures and their response to extreme pressures in MGs, as better control of properties requires a deeper understanding of the structural changes induced by the pressure.

The most fundamental studies of the MGs had to be conducted with formers of two or more elements in which the main constituents have a negative enthalpy of mixing and distinct atomic sizes [25]. Glass formation remains a challenge in monatomic systems, even in computer simulations because of these systems' shallow glass-forming ability, resulting from their fast nucleation and crystal growth kinetics. In the same context, Bhat *et al* [26] showed that the vitrification of pure monatomic MGs requires extremely high critical cooling rates, far above the experimentally accessible level, to suppress crystal growth in which the vitrification of pure metallic germanium liquid is obtained under hydrostatic pressure above 7.9 GPa. Recently, Yin *et al* [27] have chosen a lanthanide-solute MG, $Al_{93}Ce_7$, with a minor Ce concentration, studied using *in situ* high-pressure synchrotron XRD, XAS, and Molecular Dynamics (MD) simulations, attributing new light on the long-sought minor alloying effect in MGs as property-tuning knobs under increasing pressure. In our previous studies, we have shown using MD simulations that the application of the pressure upon cooling of Al-Ni-Co alloy leads to considerable changes in the structure, including the formation and the growth of nanoscale crystals in the amorphous matrix leading to the evolution of the heterogeneity of this system with pressure [28–30].

Many recent studies have reported on developing Tantalum-based materials for a broad spectrum of engineering and functional applications [31]. Compared to other materials, Tantalum (Ta) is an element exceptionally having a density of $16.65 g.cm^{-3}$, Young's modulus of $186 GPa$, bulk modulus of $200 GPa$, and high melting point ($3290 K$) [32]. Most of the research on Ta-based BMGs was conducted by Na *et al* [33], in which they used Ta as a minor addition element to tailor the GFA and properties of various BMGs. They reported that the substitution or addition of Ta in Zr-based BMGs could help precipitate crystal particles, leading to superior mechanical performances [33]. However, it has been found that Ta pure metallic liquids are succefully vitrified to form metallic glasses at a high liquid-quenching rate of 10^{14} K s^{-1} [34].

Despite the importance of the previous studies, the analysis of the effect of pressure on the atomic network and packing extended from the SRO to MRO of metallic glasses, particularly the monatomic ones, has remained problematic mostly because of their pronounced and inherent disorder and lack of suitable experimental probes. In this paper, we use MD simulations to study the atomic structure and icosahedral connectivity in a Ta MG produced under P ranged from 0 to $70 GPa$. The obtained local atomic structure was determined by means of Radial Distribution Function (RDF), Voronoi Analysis (VA) and Coordination Numbers (CN). In addition, the connections types between the perfect icosahedral-like clusters are also investigated to demonstrate the effect of P on the MRO. We found that under the application of P during the quenching process of Ta liquid, relevant structural changes was induced in the SRO and MRO of the obtained Ta MG. This revealed a significant formation of crystal-like clusters, implying the perspective of the possible crystallization of the obtained MG under P. The analysis of the MRO show the dominance of the edge-sharing in the higher P attribute the more flexible is. We present in this work a new insight into the understanding of pressure induced atomic structural rearrangement across the SRO and interconnectivity of MRO in glasses including MGs.

Simulation method

MD simulations were performed using the LAMMPS code [35]. Initially, 128000 atoms were placed in a BCC structure with periodic boundary conditions applied in all directions. An initial mean velocity corresponding to $300 K$ was given to the system following the Maxwell–Boltzmann distribution. The equations of motion were solved using the velocity-Verlet algorithm as implemented in LAMMPS with a timestep of $1 fs$. The system was heated from $300 K$ to $5000 K$ using a heating rate of $100 K/ps$ and zero pressure in NPT (constant Number of particles, Pressure, and Temperature) ensemble. Keeping the temperature fixed at $5000 K$, the pressure was increased gradually over a period of $1 ns$ from $0 GPa$ to the desired hydrostatic pressure. The system was held at the final pressure at a high temperature for $100 ps$ in NPT ensemble. Then the liquid was cooled under hydrostatic pressure from $5000 K$ to $300 K$ using a cooling rate of $100 K/ps$. At $300 K$, the hydrostatic pressure was released during a $100 ps$ run in the NPT ensemble, and the hydrostatic pressure-free glasses were further equilibrated at the same temperature without any pressure for 3 ns. Finally, a $200 ps$ simulation in the NVT (constant Number of particles, Volume, and Temperature) ensemble was performed for statistical averaging, which was performed on 200 configurations each separated by 1 ps. Nosé–Hoover thermostat and barostat were used to control temperature and hydrostatic pressure. In fact, we have chosen to cool down our system with a sufficiently high cooling rate of 100 K ps^{-1}, which is the cooling rate reported for the vitrifcation of Ta

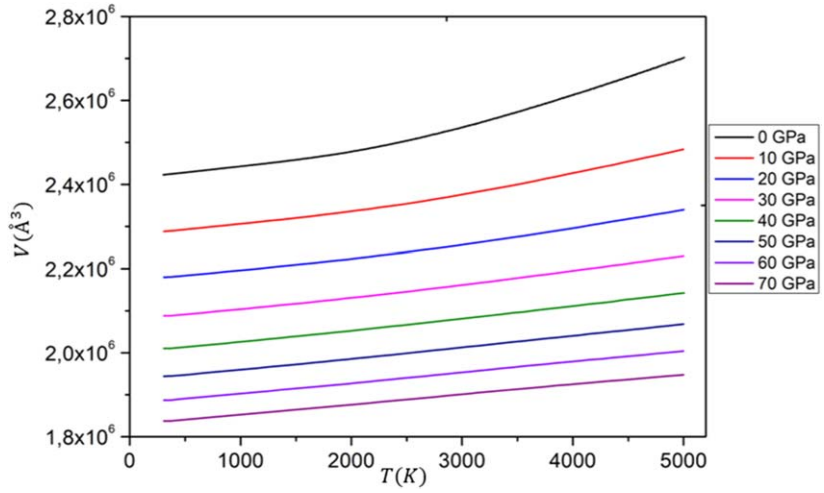

Figure 1. Volume as function of temperature during the glass formation of Ta MG for different pressures.

monatomic MG in experiments. Snapshots of the atomic structure of the studied glasses are visualized by OVITO [36].

In this work, the prototype MG former Ta is used as an example to illustrate structural ordering in MGs under applying pressure during the glass formation. To simulate Ta MG, we adopted the realistic EAM interatomic potential [34, 37], in which the potential energy landscape was fitted through extensive *ab initio* calculations based on the density functional theory. This potential has been proved to successfully capture over more than 600 reference configurations (each configuration contains 96 to 128 atoms) such as liquid phases and inherent structures, equations of state of crystal structures, point and interfacial defects and Ta MGs obtained at various cooling rates [34]. Figure 1 illustrates the MD simulation results of the Volume as function of Temperature ($V - T$) during the formation of Ta MG cooled under different pressures varying from 0 to 70 GPa. During the cooling process, the volume of the system decreases with decreasing temperature, which also decreases under compression. No obvious change has been observed in the slope of the $V - T$ curve during the cooling process, indicating the glass formation and no crystallization occurs under compression.

The atomic structure for different pressures were analyzed by employing means of RDF, VA and CN. In the structural VA, the polyhedron contains four types of polygons: triangle, tetragon, pentagon, and hexagon [38]. The triangle, tetragon, and hexagon faces have the local translational symmetry feature, while pentagon faces reflect the fivefold symmetry [39]. To quantify the average degree of five-fold symmetry present in Ta MG under P, a structural parameter W is calculated, defined as:

$$w = \sum_i (f_i^5 \times P_i)$$

Where

$$f_i^5 = n_i^5 / \sum_{k=3,4,5,6} n_i^k$$

Here P_i is the fraction of polyhedron type i and f_i^5 denotes the fraction of k-edged polygon in VP type i, while n_i^k represents the number of k-edged polygons in Voronoi polyhedron type i [40].

Results and discussion

Figure 2(a) shows the RDF, which is defined as the two-point correlation function of variation of density as a function of distance from a reference particle [41], in the Ta MG the various pressures. It can be seen from the RDF that the profile of the second nearest-neighbor shell presents the most prominent structural variations under compressing. While the splitting of the second peak into two sub-peaks becomes more pronounced, indicating crystalline grains start to form as the pressure increases. This is consistent with pressure-driven crystallization [14, 28, 29]. The height of the second sub-peak increases with pressure while it decreases for the first sub-peak. The splitting describes the atomic packing beyond the nearest neighbors, reflecting how the neighboring SROs connect and construct the MRO. We reported in our previous studies that the first and second sub-peaks correspond respectively to the formation of the face sharing and vertex sharing [42]. This could indicate that the connection schemes that relate to any two clusters may have changed under increasing

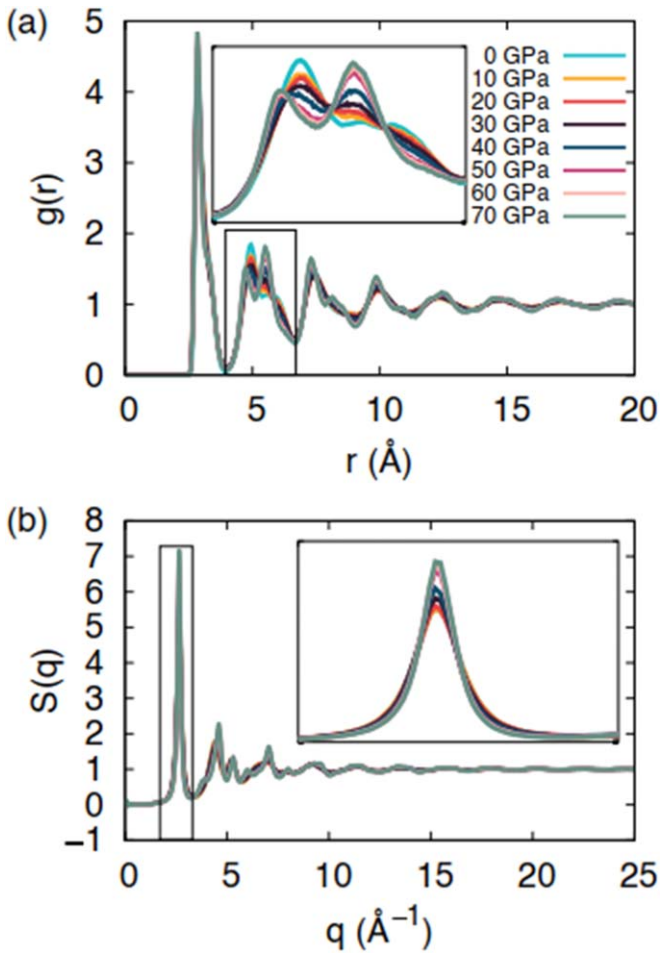

Figure 2. Structural evolution of the Ta MG during compression in the real and reciprocal spaces, (a) the RDF and (b) S(q) for pressures ranging from 0 to 70 GPa.

pressure. In order to get more direct information on MRO in reciprocal space, the structure factor ($S(q)$), which is the two-point correlation function of the Fourier component of the microscopic density [43], is also obtained as shown in figure 2(b). All the $S(q)$ curves for different pressures show similar behavior, with the exception of some changes in the shape of peaks and a too small shift towards higher q. We can see that during compression, the height of all peaks increase revealing the increase of atomic ordering in the obtained system. Increasing P causes the particles to move closer, i.e. the most probable interparticle spacing decreases. These features in the RDF and $S(q)$ reveal that when the pressure increases upon cooling reveal apparent atomic rearrangement in SRO and even extend into medium-range order MRO that could affect the physical properties to tune and open up an avenue toward unexplored space for MG design and development.

The primary information about the structure of MG is generally derived from the $S(q)$, which could be calculated using primary diffraction data or MD simulation [44]. Compared to the structural information reflected by the fluctuations at a higher q range of $S(q)$, it is suggested that the first peak can reveal more structural information and is widely studied as characteristics of MRO [45]. The position of the First Sharp Diffraction Peak (FSDP) (q_1) reflects the atomic arrangement with characteristic distance calculated as $\frac{2\pi}{q_1}$ while the full width half maximum (FWHM), which is extracted using a Gaussian fitting, is defined as resulting from the regions of atomic density fluctuation with a correlation length of $\frac{2\pi}{FWHM}$ [46]. As shown in figure 3, It is found that the corresponding *FWHM* decreases upon compressing, which reveals a decrease of structural disordering and as consequence a smaller Glass Forming Ability (GFA) within the obtained system [47–49]. In the same context, a systematic increase is observed for the correlation length, which is obviously normal since this latter is determined using the *FWHM*. The same behavior is observed for the Al-Ni-Co MG which was obtained using the rapid quenching under the same ranging pressures [28]. This leads to say that a shorter *FWHM* indicates a larger correlations length, and thus an ordered arrangement of structural units can be retained over the length scale of the MRO, attributing that the amorphous structure remains statistically more ordered under the increase of pressure.

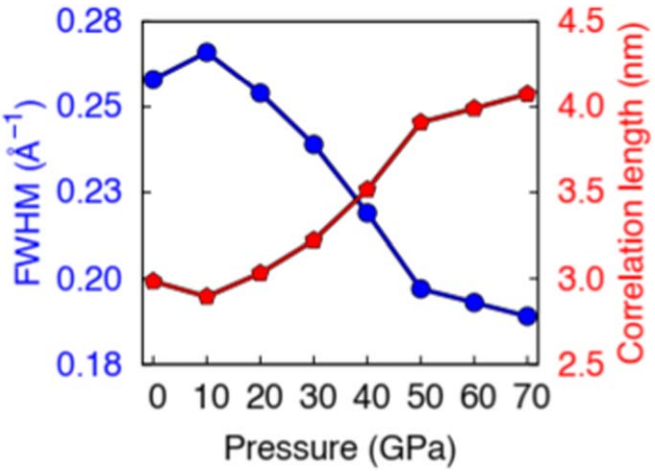

Figure 3. FWHM and correlation length as a function of the pressure.

Structure analysis of both experiments and simulations has revealed that the SRO of metallic glasses is often described by the presence of icosahedral structures, i.e., a center atom enclosed by 12 atoms, which control many physical properties in these systems [50, 51]. Although the atomic structure can be defined through the VA based on the following criteria: the lines that connect the central atom and its nearest neighbors are bisected using a set of planes, constructing thus a polyhedron [38, 52]. Each polyhedron i is recognized using the Voronoi index $<n_i^3,\ n_i^4,\ n_i^5,\ n_i^6>$ in which n_i^j ($j = 3,4,5,6$) presents the number of j-edged polygon in Voronoi Polyhedron (VP) i [38, 52]. Figure 4 shows the response of the structural atomic packing at SRO in Ta MG to the external pressure ranging from 0 GPa to 70 GPa. Here, the VP is divided, according to the study of Hwang *et al* into three categories : $\langle 0,0,12,\ n\rangle$, $\langle 0,1,10,\ n\rangle$ *and* $\langle 0,2,8,\ n\rangle$ identified as icosahedral-like VP, $\langle 0,3,6,\ n\rangle$ *and* $<\langle 0,3,7,\ n\rangle$ as mixed-like VP and, finally, $\langle 0,4,4,\ n\rangle$, $\langle 0,5,2,\ n\rangle$ *and* $\langle 0,6,0,8\rangle$ as crystal-like VP, in which n is typically ranged from 0 to 6 [53]. For clarity, we choose to display the most relatively higher population VP. The Ta MG (300 K) at 0 GPa has a VP distribution dominated by the icosahedral-like cluster of $\langle 0,1,10,2\rangle$, whereas at 70 GPa, the distribution has changed to be dominated by the crystal-like cluster of $\langle 0,6,0,8\rangle$ with a population of *24.8%*. More precisely, the content of all the icosahedral-like clusters decreases while that of crystal-like VP increases with increasing pressure. However, the pressure dependence of the mixed-like VP including $\langle 0,\ 3,6,\ 4\rangle$, $\langle 0,\ 3,6,\ 5\rangle$ and $\langle 0,\ 3,6,\ 6\rangle$ shows a maximum at $P = 30GPa$. This pointed on the fact that the local structural arrangement shows a strong correlation with applying external pressure. The significant increase of 14-coordinated crystal-like VPs of $\langle 0,\ 4,4,\ 6\rangle$ which presents the Face Centered Center (FCC) structure, and $\langle 0,\ 6,0,\ 8\rangle$ presenting the body-centered cubic (BCC) structure could be attributed to that the crystallization occurs under the application of P [54]. The maximum exhibited on the mixed like clusters is explicitly due to a structural crossover in SRO at 30*GPa*. The same behavior is identified when studying the structural evolution of the high entropy metallic glass $Ti_{16.7}\,Zr_{16.7}\,Hf_{16.7}\,Cu_{16.7}\,Ni_{16.7}\,Be_{16.7}$ in pressure ranges from 0 to 40*GPa*, in which detailed analysis of the first sharp peak of $S(q)$ and $g(r)$ reveals a crossover at 20*GPa* [55]. This crossover is attributed to the competitive transformation of icosahedral-like clusters to crystal-like ones since the crystal nucleation in glasses is found to be influenced by the degree of five-fold symmetry or the content of icosahedra. This leads to the conclusion that the mixed-like clusters can be regarded as an intermediate state from the icosahedral-like to the crystal-like including the FCC and BCC structures. However, this supports the finding of Hu and Tanaka, reporting the formation of two type locally favored orderings in multicomponent metallic liquids: the icosahedral and crystal-like bond orientational orderings [56]. Their results demonstrate that the competitive formation between these local structures plays crucial in determining the GFA by affecting the thermal energy–scaled interface energy [56]. Figure 5 displays three slices of the local atomic orderings in the three dimensional space at 300 K under three different pressures conditions 0, 40, 70 GPa. It can be seen that the cooling under P induce the formation of crystalline grains of BCC structures. The size and the content of these crystalline grains increase with increasing P. The formation of the crystalline ordering in the glassy state of various pressures, can be also identified using the Common Neighbor Analysis (CNA) technique as listed in table 1. Under increasing pressure during the cooling process of Ta MG, the content of icosahedral configuration decreases, to be replaced by an increase of BCC configuration with a fraction of 24.1% , which is in accordance with the results reported by the VA method.

The CN can be used to determine the local atomic SRO, which plays an important role in the structure and stability of glassy materials and, thus, controls the physical and mechanical properties [57–60]. The CN can be determined using the integration of the RDF up to its first minimum. Figure 6 shows the total CN at 300 K from

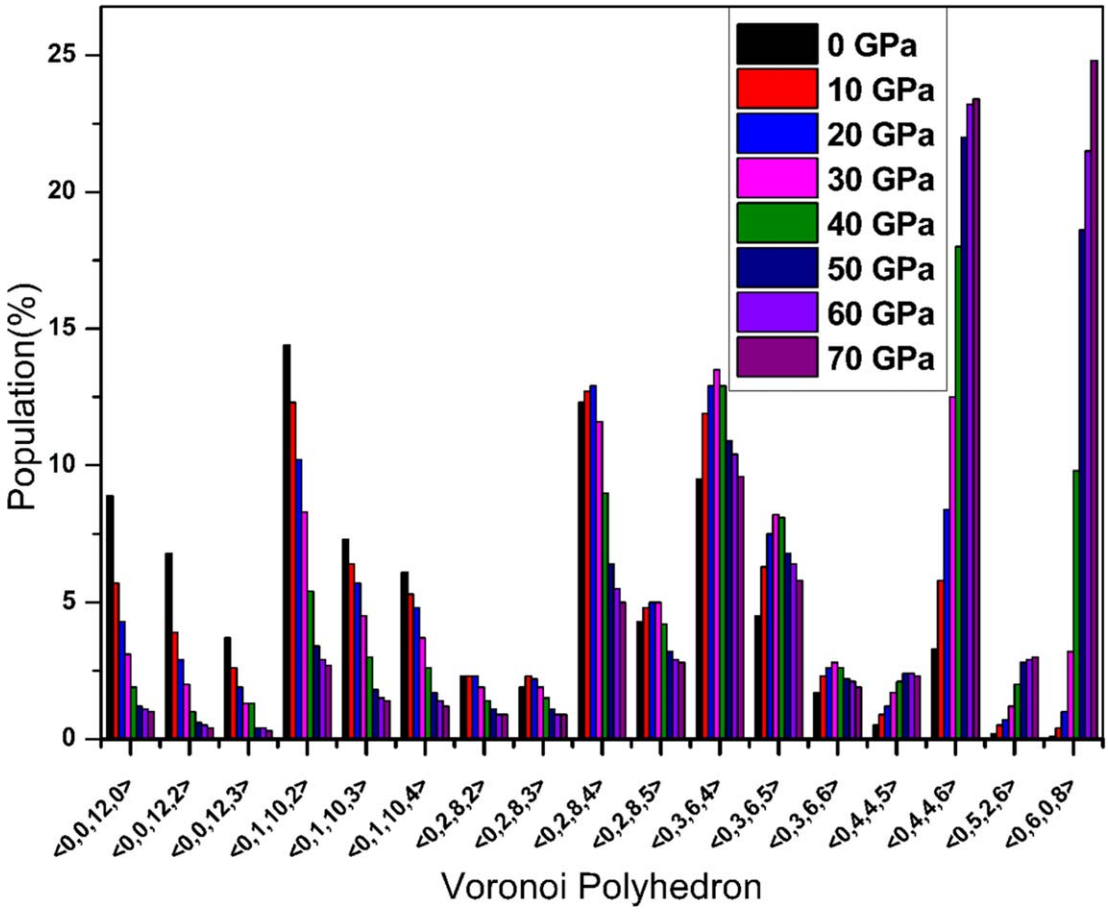

Figure 4. Pressure dependence of the Voronoi polyhedron, including icosahedral-like, mixed-like, and crystal-like clusters in Ta MG.

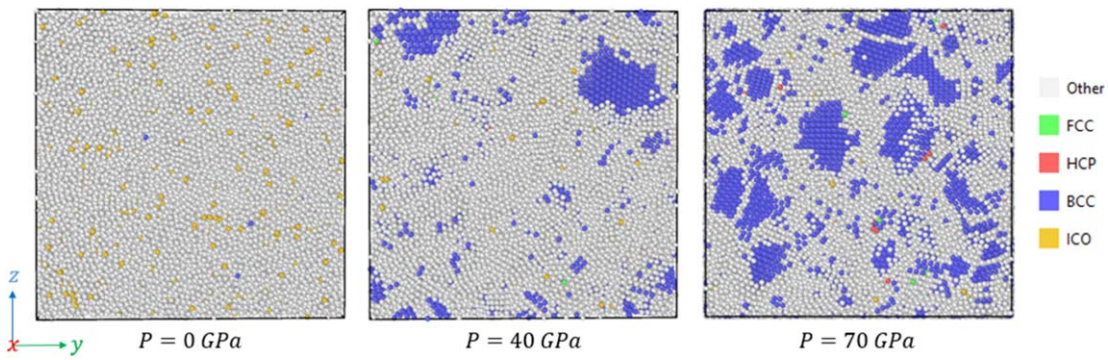

Figure 5. Snapshots of Ta MG at three different pressures 0, 40, 70 GPa.

Table 1. results of CNA for Ta MG at different pressures.

P(GPa)	0	10	20	30	40	50	60	70
ICO	3.4	1.9	1.4	1	0.5	0.3	0.3	0.2
BCC	0.1	0.3	0.8	2.9	9.2	17.8	20.8	24.1
HCP	0	0	0	0	0	0.1	0.1	0.1
FCC	0	0	0	0	0.1	0.1	0.1	0.1
Others	96.5	97.8	97.8	96.1	90.2	81.7	78.7	75.5

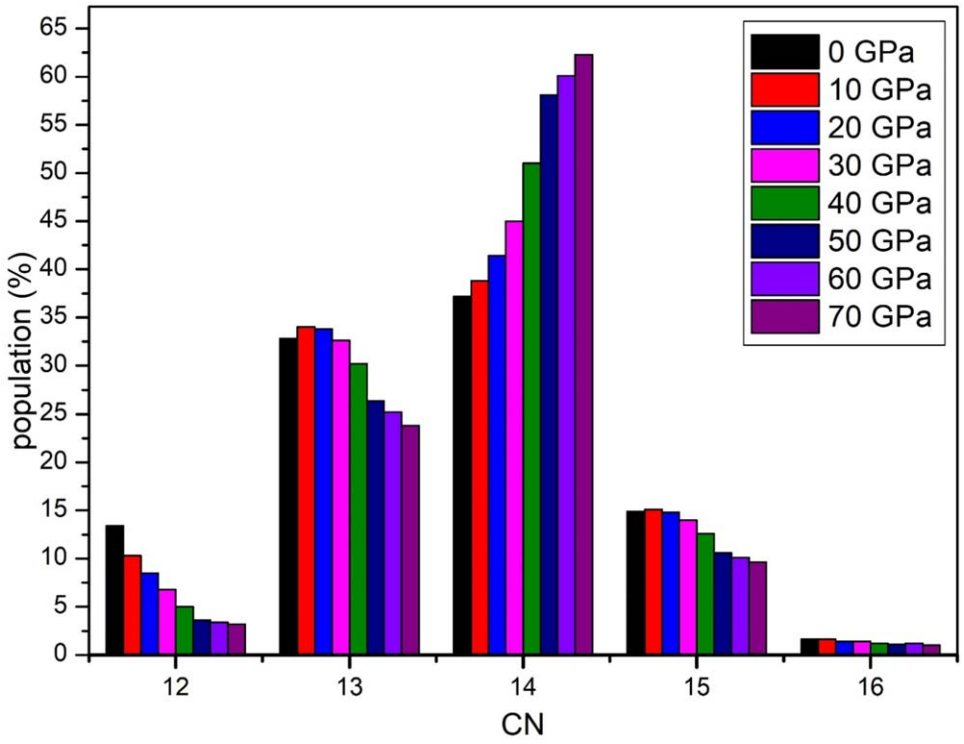

Figure 6. Population of the most dominant CN in Ta MG obtained at different pressures.

0 to 70*GPa*. The profile of the total CN demonstrates that the most prominent CN in all samples is 14. Meanwhile, the proportion of all CN increases with the increase of P, reaching 62,3 % for $CN = 14$ in the glassy state of 70*GPa*. This observation is also confirmed within the analysis of Voronoi, in which a remarkable increase of crystal-like cluster of $\langle 0,4,4,6 \rangle$ of $CN = 14$ is observed. The results illustrated for CN indicate that applying P during the quenching process induces a changing ordering in local atomic packing. It suggests that further compression of metallic liquids is expected to further promote the SRO in the obtained MG.

We demonstrated in our previous studies using MD simulations based on Voronoi structural analysis that the dominant SRO in MGs, including Monatomic and multicomponent systems, is the icosahedral-like cluster of $\langle 0,1,10,2 \rangle$, in which their packing gives rise to a distinct MRO [42, 45]. This Icosahedral SRO and local atomic symmetry, including the local fivefold and translational symmetries, play an essential role in MGs' dynamics and mechanical properties. The fivefold symmetry can capture the structural evolution during the glass formation, and proves to be the result of the evolution of both the rotational and long-range translational symmetries during the vitrification process [39]. We can see from figure 7 that W decreases with increasing *P*. This is consistent with our previous studies performed for the AlNiCo MG. However, different phenomenon is observed in the study of Hu *et al* [61], in which MD simulations was carried out to to study the structure and dynamics of a ternary metallic glass-forming liquid subjected to high pressures. For pressures ranging from 0 to 18 GPa, Hu *et al* [61] demonstrated the enhanced behaviour of the five-fold symmetry during the cooling process and compressing, which is due to squeezing out the free volume and favoring local coordination induced by high pressures. In general, decreasing W indicates that the nucleation is enhanced since the homogenous freezing in the supercooled liquid is attributed to a competitive formation between fivefold symmetric and crystalline structures [39]. Increasing the fivefold symmetry affects the thermodynamics and the system's kinetics, exhibiting these features: a) the freezing can be suppressed, and the fluid-solid phase boundary moves to higher pressures and densities [62]. The crystalline nucleation under the application of P during the quenching process, identified also as the increase of BCC and FCC VPs, i.e., $\langle 0,6,0,8 \rangle$ and $\langle 0,4,4,6 \rangle$, is strongly depended to fivefold symmetry and provides insights into considering the P as a novel way of enhancing crystalline ordering in the glass formers.

To extract the structural information on the 3D atomic configurations that the conventional methods from atomic configurations cannot sufficiently analyze, we have calculated Bond Angle Distributions (BAD) with increasing pressure, as shown in figure 8. It is observed that the distribution of bond angles at higher P is distinctively different from those at lower P, indicating that the structure of Ta MG under high pressure is very different from that at ambient pressure. At 0*GPa*, the BAD shows three maximums almost close respectively to

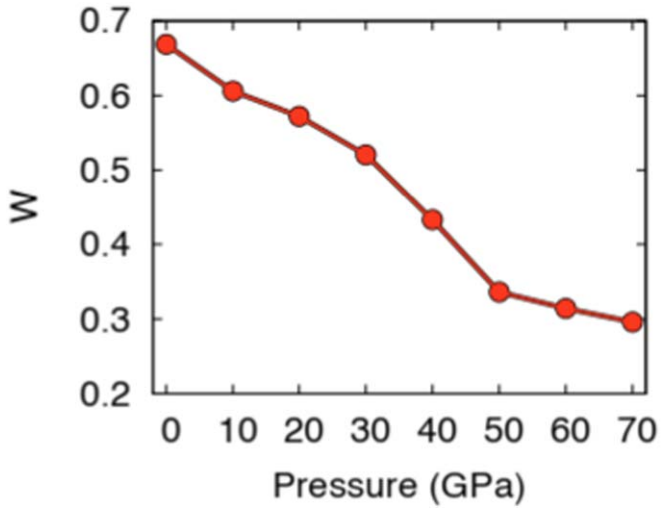

Figure 7. Structural indicator of the fivefold symmetry as a function of pressure.

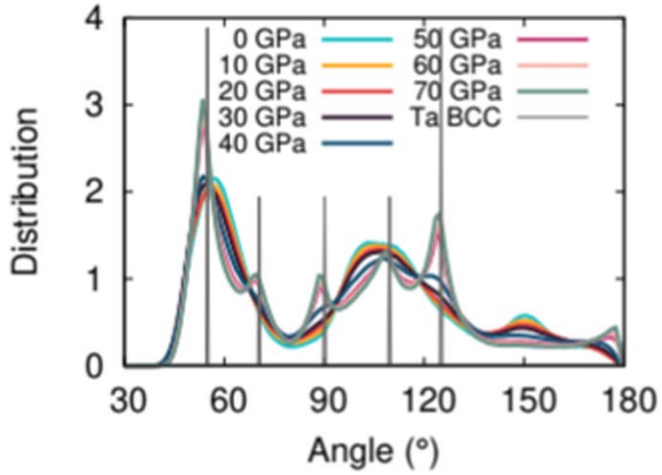

Figure 8. BAD for the obtained glassy states at 0, 10, 20, 30, 40, 50, 60, 70 GPa and Ta BCC.

60°, 110°*and* 150°. With increasing P, the 1st maximum peak position gradually gets smaller down to 46° with a shoulder peak, while the *FWHM* of the 2nd maximum decrease with 2 shoulder peaks and the distribution of the 3rd maximum becomes distorted to show a peak at around 180°. Angles around 60°*and*120° would result from the formation of the icosahedral clusters that may belong to the packing of tetrahedra, which are composed of nearly equilateral triangles, whereas the peak formed at around 180° could reflect the linear chains of nearest neighbor connected icosahedra. The increasing height of the 1st peak indicates an increasing icosahedral structure upon compressing. In the same context, increasing P causes sharper shoulder peaks at positions similar to that of crystallized Ta, suggesting that the local order starts to become a BCC. We note that the number of cubic clusters, including the BCC, increases as the P increases, leading to confirmation that the ordering increases when the liquid is cooled under high pressure.

Developing the local connectivity of the SRO environments and therefore begin to probe MRO, is also an important key factor to understand the effect of P and the rapid solidification process. Besides the BAD, an alternative way to investigate the MRO under HP in Ta MG is to examine the spatial correlation of the SRO clusters to see how a network is formed by these clusters in the glass [63]. There are four different types of connections between two SRO clusters, i.e., vertex-sharing (Versus) (sharing one atom), edge-sharing (ES) (sharing two atoms), face-sharing (FS) (sharing three to four atoms), and inter-penetrating sharing (IS) (sharing five atoms) [64]. Figure 9 plots the content of the four types of connectivity, including Versus, ES, FS, and IS as a function of P. We note that the content of each connection type is computed by only considering the interconnectivity between perfect icosahedral-like clusters of $\langle 0,0,12,0\rangle$. It is clearly observed that increasing P induces a significant change in the population of cluster connectivity types. At 0*GPa*, the Versus has the

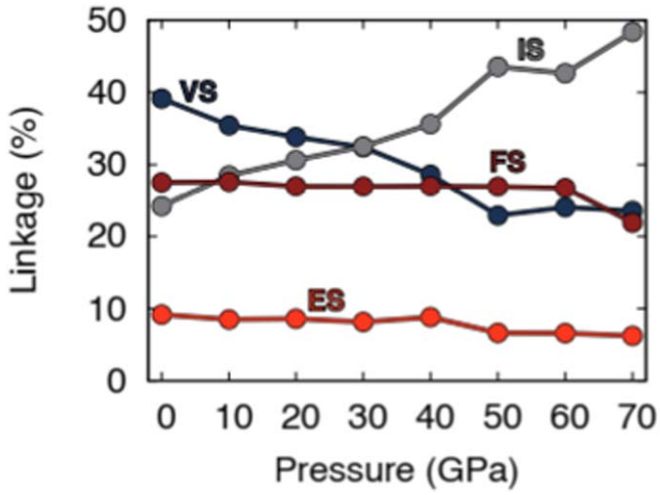

Figure 9. Fraction of the connectivity types between <0,0,12,0> in Ta MG for different pressures.

maximum content, but rapidly decrease because of the increase in the number of IS, whilst the population of ES and FS remain largely unchanged. As the P increases, The IS eventually dominates the Ta MG, which could be attributed to the higher density of the icosahedral clusters in this sample. However, Ding *et al* [65] reported that FS is the most dominant connection type during the cooling process from a liquid state to a glassy state of $Cu_{64}Zr_{36}$ MGs, exhibiting the stiffest elastic response contrary to the IS, which has an elastic response. In other words, a sample exhibiting clusters with more FS would result in higher stiffness, while those with more IS would show better flexibility.

Conclusion

The atomic structural features of monatomic Ta MG under increasing pressure were investigated by MD simulations based on the EAM potential. The structures of the eight obtained glassy states were characterized by (1) the RDF and $S(q)$, (2) the *FWHM* of the 1st peak and the correlation length change, (3) the fraction change of the local fivefold symmetry average degree (4) the BAD change, and, finaly, (5) the fraction of the four types of polyhedra connection. We show using the calculated RDF and $S(q)$ for various pressures, that a specific atomic rearrangement in the SRO and MRO structures is identified, indicating crystalline grains start to form as the pressure increases. The correlation between the *FWHM* of the first peak of the $S(q)$ and the correlation length indicates that the obtained amorphous structure remains statistically more ordered under varying P. We demonstrated in this work that the full icosahedra $\langle 0,0,12,0\rangle$ and the distorted icosahedra $\langle 0,1,10,2\rangle$ are the main structures in Ta MG of 0 GPa. With increasing pressure, the content of icosahedral order decreases, to be replaced by an increase and domination of crystal-like cluster $\langle 0,4,4,6\rangle$, while that of the mixed-like clusters shows a maximum at $P = 30GPa$. The maximum exhibited on the mixed like clusters is found to be due to a structural crossover in SRO at $30GPa$, leading to say that the mixed-like clusters can be regarded as an intermediate state of the structural transformation from the icosahedral-like to the crystal-like including the FCC and BCC structures. The results derived in the CN analysis suggest that applying pressure during the quenching process of Ta MG favors the short-range ordering in the obtained Ta MG. However, the decrease of icosahedral order is accompanied by a decrease of the local fivefold symmetry under compression, which is responsible for the beginning of the crystalline grains formation in the obtained atomic structures. This is also confirmed within the findings of the BAD, including the formation of BCC structures. The applied pressure increases the fraction of inter-penetrating sharing, increasing the system's flexibility. These results provide a theoretical basis for understanding the evolution in short- and medium-range order under pressure in metallic glasses, suggesting that applying pressure promotes the flexibility of monatomic Ta MG.

Data availability statement

The data cannot be made publicly available upon publication because they are not available in a format that is sufficiently accessible or reusable by other researchers. The data that support the findings of this study are available upon reasonable request from the authors.

ORCID iDs

Meryem Kbirou https://orcid.org/0009-0006-0432-1663

References

[1] Inoue A 1995 *Mater. Trans.* **36** 866–75
[2] Inoue A and Takeuchi A 2011 *Acta Mater.* **59** 2243–67
[3] Zhang W, Inoue A and Wang X M 2008 *Rev. Adv. Mater. Sci.* **18** 1–9
[4] Dambatta M S, Izman S, Yahaya B, Lim J Y and Kurniawan D 2015 *J. Non-Cryst. Solids* 426 (Elsevier B V) 110–5
[5] Inoue A and Takeuchi A 2011 *Acta Mater.* **59** 2243–67
[6] Chen H S 1980 Glassy metals *Reports Prog. Phys.* **43** 353–432
[7] Cheng Y Q and Ma E 2011 *Prog. Mater Sci.* 56 (Elsevier Ltd.) 379–473
[8] Sheng H W, Ma E and Kramer M J 2012 *JOM* **64** 856–81
[9] Sheng H W, Luo W K, Alamgir F M, Bai J M and Ma E 2006 *Nature* **439** 419–25
[10] Zhou Z-Y, Yang Q and Yu H-B 2024 *Prog. Mater Sci.* **145** 101311
[11] Li S, Zhang J C and Sha Z D 2020 *J. Alloys Compd.* **848** 1–6
[12] Wu Y *et al* 2021 *Nat. Commun.* **12** 1–9
[13] Miao M, Sun Y, Zurek E and Lin H 2020 *Nature Reviews Chemistry* **4** 508–27
[14] Zeng Q S *et al* 2007 *Proc. Natl Acad. Sci.* **104** 13565–8
[15] Du T, Sørensen S S, To T and Smedskjaer M M 2022 *J. Appl. Phys.* **131** 170901
[16] Ouldhnini Y, Atila A, Ouaskit S and Hasnaoui A 2021 *Phys. Chem. Chem. Phys.* **23** 15292–301
[17] Ouldhnini Y, Atila A, Ouaskit S and Hasnaoui A 2022 *J. Non. Cryst. Solids* **590**
[18] Bakhouch Y *et al* 2024 *J. Am. Ceram.* **107** 4572–84
[19] Phan A D, Zaccone A, Lam V D and Wakabayashi K 2021 *Phys. Rev. Lett.* **126**
[20] Lou H B *et al* 2014 *J. Acta. Materialia.* **81** 420–7
[21] Wang C *et al* 2017 *Appl. Phys. Lett.* **110.** 111901–5
[22] Luo Q *et al* 2015 *Nat. Commun.* **6.** 5703
[23] Lou H *et al* 2020 *Nat. Commun.* **11** 314.
[24] Wang W H, He D W, Zhao D Q, Yao Y S and He M 1999 *Appl. Phys. Lett.* **75** 2770–2
[25] Cheng Y Q, Ma E and Sheng H W 2009 *Phys. Rev. Lett.* **102** 1–4.
[26] Bhat M H *et al* 2007 *Nature* **448** 787–90
[27] Yin Z, Lou H, Sheng H, Zeng Z, Mao W L and Zeng Q 2021 *J. Appl. Phys.* **129** 025108
[28] Atila A, Kbirou M, Ouaskit S and Hasnaoui A 2020 *J. Non. Cryst. Solids* **550** 120381
[29] Kbirou M, Hasnaoui A, Saadouni K, Badawi M and Mazroui M 2019 *Comput. Mater. Sci.* **166** 20–9
[30] Mo Y *et al* 2020 *Phys. Chem. Chem. Phys.* **22** 18078–90
[31] Bharath K, Chelvane J A, Kumawat M K, Nandy T K and Majumdar B 2019 *J. Non. Cryst. Solids* **512** 174–83
[32] Meng D *et al* 2011 *J. Non. Cryst. Solids* **357** 1787–90
[33] Na J H, Park J M, Han K H, Park B J, Kim W T and Kim D H 2006 *Mater. Sci. Eng. A* **431** 306–10
[34] Zhong L, Wang J, Sheng H, Zhang Z and Mao S X 2014 *Nature* **512** 177–80
[35] Thompson A P *et al* 2022 *Comput. Phys. Commun.* **271** 108171
[36] Stukowski A 2010 *Model. Simul. Mater. Sci. Eng.* **18** 085001
[37] Daw, M. S. and Baskes, M. I. 1984 *Physical Review B* **29** 6443
[38] Hu Y C, Li F X, Li M Z, Bai H Y and Wang W H 2015 *Nat. Commun.* **6** 8310
[39] Taffs J and Royall C P 2016 *Nat. Commun.* **7** 13225
[40] Li M Z, Peng H L, Hu Y C, Li F X, Zhang H P and Wang W H 2017 *Chinese Physics* B **26,** 016104.
[41] Zhao H, Zhao D, Zhu B and Wang S 2018 . *In Metallic Glasses-Properties and Processing.* (IntechOpen.) (https://doi.org/10.5772/intechopen.76830)
[42] Kbirou M, Trady S, Hasnaoui A and Mazroui M 2017 *Philos. Mag.* **6435** 1–19
[43] Tanaka H, Tong H, Shi R and Russo J 2019 *Nat. Rev. Phys.* **1** 333–48
[44] Popescu M A 2005 *J. Ovonic Res.* **1** 7–19
[45] Kbirou M, Mazroui M and Hasnaoui A 2018 *J. Alloys Compd.* **735** 464–72
[46] Makarov A S *et al* 2023 *Intermetallics* **163** 108041
[47] Joress H *et al* 2020 *ACS Comb. Sci.* **22** 330–8
[48] Li M X *et al* 2022 *Nat. Mater.* **21** 165–72
[49] Nelli D, Roncaglia C and Minnai C 2023 *Adv. Phys. X* **8** 2127330
[50] Amigo N, Palominos S and Valencia F J 2023 *Sci. Rep.* **13** 1–10
[51] Zhang X *et al* 2023 *Proc. Natl Acad. Sci.* **120** e2302281120
[52] Sayad S, Khanzadeh M, Alahyarizadeh G and Amigo N 2023 *Sci. Rep.* **13** 16109
[53] Hwang J 2011 Nanometer scale atomic structure of zirconium based bulk metallic glass *Diss.*
[54] Pan S P, Feng S D, Qiao J W, Wang W M and Qin J Y 2015 *Sci. Rep.* **5** 1–8
[55] Zhang X *et al* 2022 *Phys. Rev.* B **105** 224201
[56] Hu Y C and Tanaka H 2020 *Sci. Adv.* **6** 1–12
[57] Kono Y *et al* 2016 *Proc. Natl. Acad. Sci. U. S. A.* **113** 3436–41
[58] Solomatova N V and Caracas R 2019 *J. Geophys. Res. Solid Earth* **124** 11232–50
[59] Yang Y *et al* 2021 *Nature* **592** 60–4
[60] Hung P K, Vinh L T, Nghiep D M and Nguyen P N 2006 *J. Phys. Condens. Matter* **18** 9309–22
[61] Hu Y *et al* 2017 *J. Chem. Phys.* **146** 024507
[62] Karayiannis N C, Malshe R, De Pablo J J and Laso M 2011 *Phys. Rev. E - Stat. Nonlinear, Soft Matter Phys.* **83**
[63] Lee M, Lee C M, Lee K R, Ma E and Lee J C 2011 *Acta Mater.* **59** 159–70
[64] Soklaski R, Nussinov Z, Markow Z, Kelton K F and Yang L 2013 *Phys. Rev. B - Condens. Matter Mater. Phys.* **87** 1–8
[65] Ding J, Ma E, Asta M and Ritchie R O 2015 *Sci. Rep.* **5** 17429